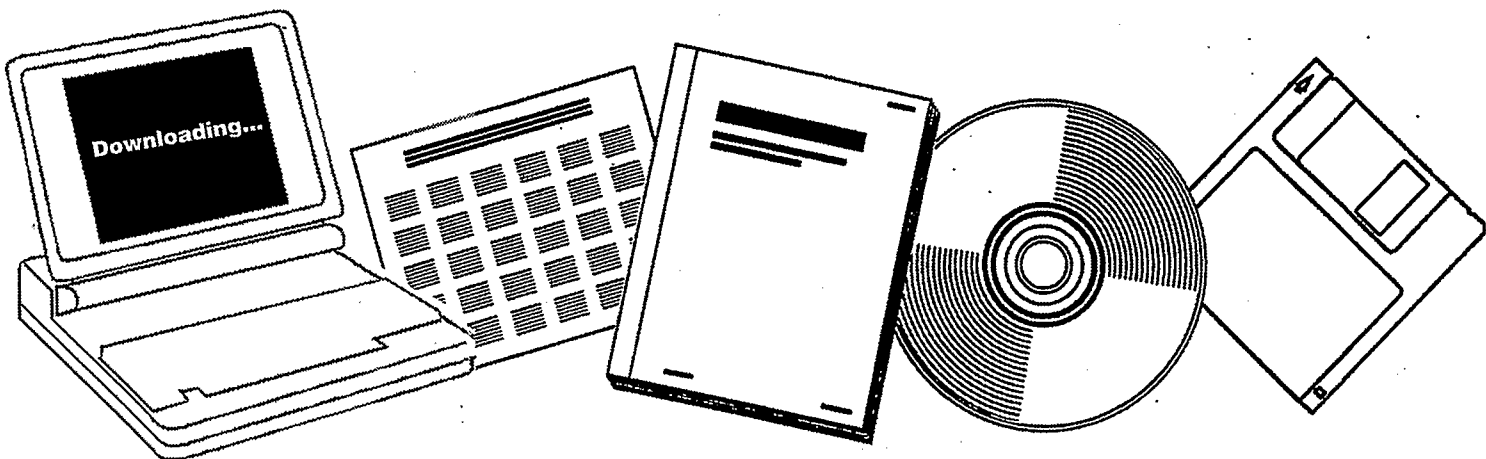# NOVEL EXPERIMENTAL STUDIES FOR COAL LIQUEFACTION: QUARTERLY PROGRESS REPORT, JULY 1, 1986 TO SEPTEMBER 30, 1986

PITTSBURGH UNIV., PA

1986

# One Source. One Search. One Solution.

●
NTiS

Providing Permanent, Easy Access to U.S. Government Information

National Technical Information Service is the nation's largest repository and disseminator of government-initiated scientific, technical, engineering, and related business information. The NTIS collection includes almost 3,000,000 information products in a variety of formats: electronic download, online access, CD-ROM, magnetic tape, diskette, multimedia, microfiche and paper.
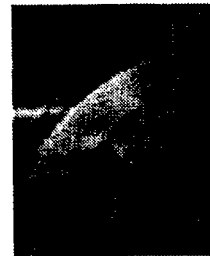
Search the NTIS Database from 1990 forward
NTIS has upgraded its bibliographic database system and has made all entries since 1990 searchable on **www.ntis.gov.** You now have access to information on more than 600,000 government research information products from this web site.

Link to Full Text Documents at Government Web Sites
Because many Government agencies have their most recent reports available on their own web site, we have added links directly to these reports. When available, you will see a link on the right side of the bibliographic screen.

Download Publications (1997 - Present)
NTIS can now provides the full text of reports as downloadable PDF files. This means that when an agency stops maintaining a report on the web, NTIS will offer a downloadable version. There is a nominal fee for each download for most publications.

For more information visit our website:

www.ntis.gov

U.S. DEPARTMENT OF COMMERCE
Technology Administration
National Technical Information Service
Springfield, VA 22161

QUARTERLY PROGRESS REPORT

NOVEL EXPERIMENTAL STUDIES FOR COAL LIQUEFACTION:

Gerald D. Holder
Yatish T. Shah
John W. Tierney

University of Pittsburgh
Pittsburgh, PA 15261

July 1, 1986 to September 30, 1986

- DISCLAIMER

MASTER

Task 1: Thermal Behavior of Slurry Reactors Used for Indirect Coal Liquefaction

The conversion of synthesis gas to liquid products is usually carried out with the reactants in the gas phase and a solid catalyst. Because of relatively poor heat transfer from the gas to the solid, the exothermic heat of reaction is difficult to remove, and care must be taken to prevent the catalyst from overheating with loss of selectivity and activity. Slurry reactors in which the catalyst is suspended in a liquid medium and the gases are bubbled through the slurry have intrinsically better heat transfer characteristics and appear promising for indirect liquefaction processes.

Scope of Work

In task 1 of this project, the thermal behavior of slurry reactors when used for indirect coal liquefaction is being studied. Previous work with a ruthenium catalyst has shown that two distinct steady states can be found for identical operating conditions. Other catalysts and operating conditions are being studied.

Work is being done using three indirect liquefaction routes involving synthesis gas -- the Fischer-Tropsch reaction, the one-step conversion to methanol, and the two-step conversion to methanol.

Results and Highlights

The experimental work during the last quarter was concentrated on determination of kinetic parameters for the reverse carbonylation reaction, an experimental study of effect of CO and CO_2 on the hydrogenolysis catalyst, and evaluation of the simultaneous two-step methanol synthesis in a single stage reactor based on the kinetic data obtained.

Using the experimental data obtained previously for carbonylation of methanol, a non-linear regression method was used to determine the kinetic parameters for the reverse carbonylation reaction. The activation energy for the reserve reaction was found to be 139.6 $\pm$ 1.1 [kJ/mole]. The average error of the regression was 7.1%. The overall reaction rate for the carbonylation of methanol using potassium methoxide catalyst at temperatures of 60 - 110°C was found to be:

$$r_1 = 4.11 \times 10^7 \exp(-10126/T) \; C_{Cata}C_{MeOH}P_{CO}$$

$$-1.70 \times 10^{17} \exp(-16788/T)C_{Cata}C_{MeF} \tag{1}$$

Comparing the present result to Tonner's results (1983) which were obtained using sodium methoxide as the catalyst, the same reaction orders to methanol, CO and catalyst were found for the forward reaction. Tonner found the activation energy of the forward reaction was 67 kJ/mole compared to 84.2 found in this work using a potassium catalyst. A comparison of rate constants for the forward carbonylation reaction is shown in Table 1 and indicates that the potassium catalyst has a higher activity than sodium catalyst, which is consistent with Tonner's finding that a lower ionization potential of an alkali metal results in a higher catalytic activity. The kinetic parameters for the reverse reaction have not been reported previously in the literature.

Table 1

Comparison of Carbonylation Rate Constants ($l^2mol^{-2}min^{-1}$)

Temperature (C)	Catalysts	
	This Study CH_3OK	Tonner CH_3ONa
50.0	0.00617	0.00330
60.0	0.01630	0.00740
70.0	0.04073	0.01433 ·

The fast carbonylation rate and fast equilibrium observed in the experiments indicate the existence of an active intermediate, which has equilibriium relations with both reactants and product. The mechanism proposed by Christiansen (1919) can be used to describe both forward and backward reactions as

$$CH_3OOCH + CH_3O^- == (CH_3OOC)^- + CH_3OH \qquad (2)$$

$$CH_3OOC^- == CH_3O^- + CO \qquad (3)$$
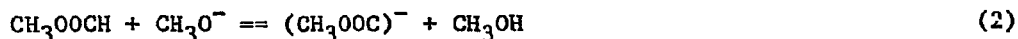
A strong equilibrium limitation on carbonylation of methanol was found. The equilibrium methanol conversion depends on temperature and is shown in Figure 1, which is calculated from Equation 1. For a reaction carried out at $80^\circ C$, as reported by Agulio and Horlenko (1980), the equilibrium conversion of methanol is about 53%. If the reaction is to be carried out simultaneously with the hydrogenolysis reaction, a higher temperature, say $120^\circ C$, is required for the hydrogenolysis. The equilibrium methanol conversion at $120^\circ C$ is only about 14%. Reported studies on hydrogenolysis are usually in the temperature range of $140 - 180^\circ C$, at which the equilibrium methanol conversion is less
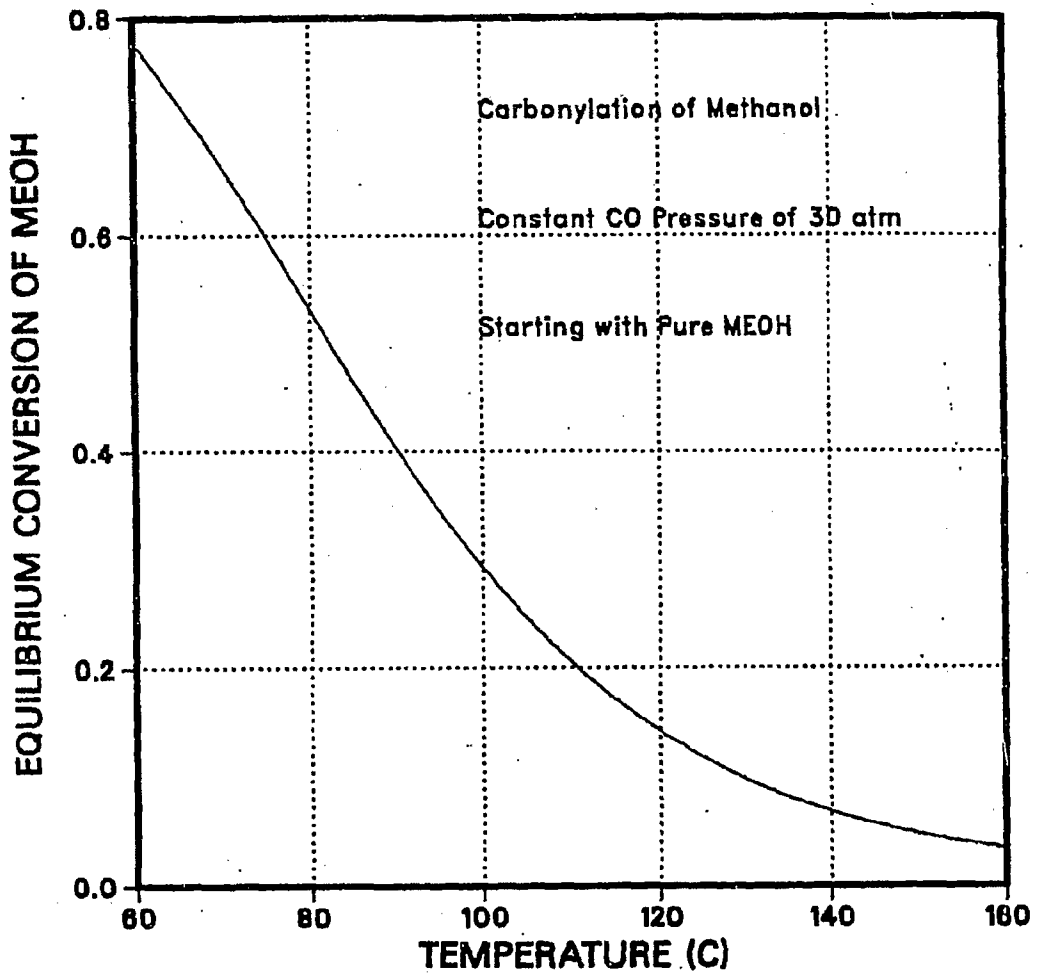
Figure 1. Dependence of equilibrium conversion of methanol
on temperature for carbonylation of methanol

than 7%. This equilibrium limitation casts some doubts about the feasibility of carrying out both reactions simultaneously in a single reactor.

Study of the effect of CO on the hydrogenolysis catalyst continued in the last quarter. A batch reaction method similar to that used for the carbonylation runs was used for these experiments. The total pressure and the liquid composition were measured and used to calculate the reaction rate. Combining the data obtained in the last quarter with those obtained for hydrogenolysis previously, a non-linear regression was used to determine the kinetic rate expression for the hydrogenolysis of methyl formate using G-89 catalyst. A power law and nine different Langmuir-Hinshelwood type rate expressions were used to fit the experimental data. The mechanism proposed by Sorum was also tried. The best fit was found to be:

$$r_2 = \frac{1871.5 \exp(-8348./T) \; C_{MeF} P_{H2} C_{Cata}}{1 + \sqrt{0.039 \; C_{MeF}} + 0.096 \; P_{CO}} \tag{4}$$

The activation energy was found to be 69.4 ± 2.0 [kJ/mole]. A comparison of the experimental and predicted reaction rates is shown in Figure 2. Average error of the regression is 10%.

Although Equation 4 is empirical, it suggests that methyl formate dissociates into two groups after being adsorbed on the catalyst surface and that the reaction occurs either between the dissociated methyl formate and hydrogen in the liquid or between the dissociated methyl formate and adsorbed hydrogen on different active sites, and the coverage of hydrogen on the catalyst surface is small. Since one methyl formate is converted into two methanols, the dissociation of methyl formate is likely. Since the hydrogenolysis reaction is carried out in a methyl formate rich atmosphere, the small coverage of hydrogen on the surface is understandable. The term for
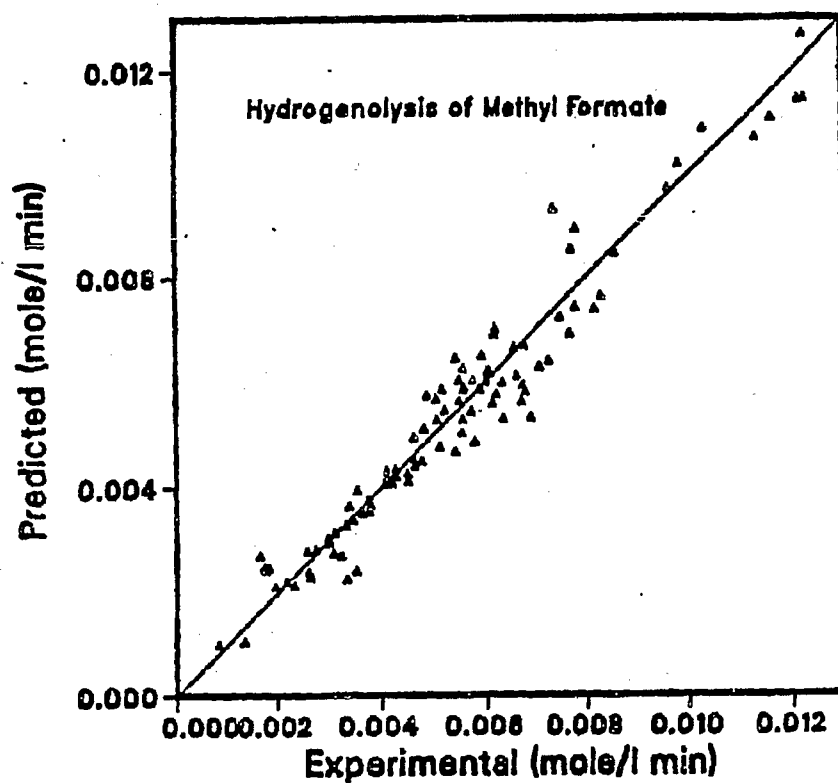
Figure 2. Comparison of predicted and experimental rate of reaction per hydrogenolysis of methyl formate.

partial pressure of CO in the denominator indicates adsorption of CO on the catalyst surface, which suggests that the inhibitory effect of CO on the hydrogenolysis rate is due to competitive adsorption of CO and methyl formate on the same active sites.

The apparent activation energy obtained in this study is somewhat higher than that obtained by Monti et al. (1986) and Sorum and Onsager (1984). This may be a result of different catalyst reduction methods as well as different ranges of reaction temperature used. A comparison of calculated reaction rates is shown in Figure 3. The rate observed in this study is comparable to that reported by Monti et al. but much lower than that of Sorum and Onsager. Gas phase catalyst reduction was employed in this study and in that by Monti et al. while a liquid phase reduction was used by Sorum and Onsager. Perhaps the differences are due to the method of catalyst reduction.

The effect of CO on the hydrogenolysis rate observed in this study is different from that reported by Monti et al. as shown in Figure 4. They found a stronger effect of CO on the hydrogenolysis reaction in the CO pressure up to 40 atm. Different catalyst reduction temperature may be partially responsible for this difference. The deleterious effect of CO was found to be partially reversible when CO was removed. The reaction rate before feeding CO to the reactor was found to be 10% higher than the rate after exposure to CO.

Since a small percentage of CO_2 is usually presented in synthesis gases, the effect of CO_2 on the hydrogenolysis was also measured. After adding 0.6% CO_2 to the reactor in the gas phase a 40% reduction in the hydrogenolysis rate was observed. The deactivation of the copper chromite catalyst by CO_2 was not reversible upon removal of the CO_2.

Rate constants for the carbonylation and the hydrogenolysis reactions are listed in Table 2 and indicate that carbonylation and decarbonylation rates
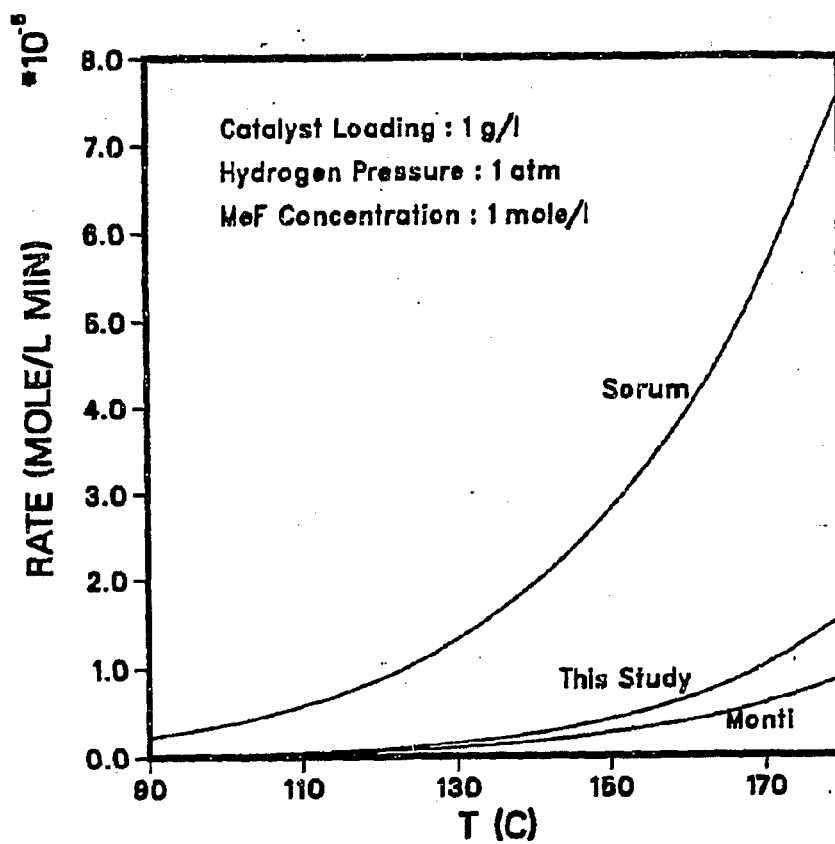
Figure 3. Comparison of reaction rates found for hydrogenolysis of methyl formate with those reported by other investigators. Catalyst is G-89 (United Catalyst).
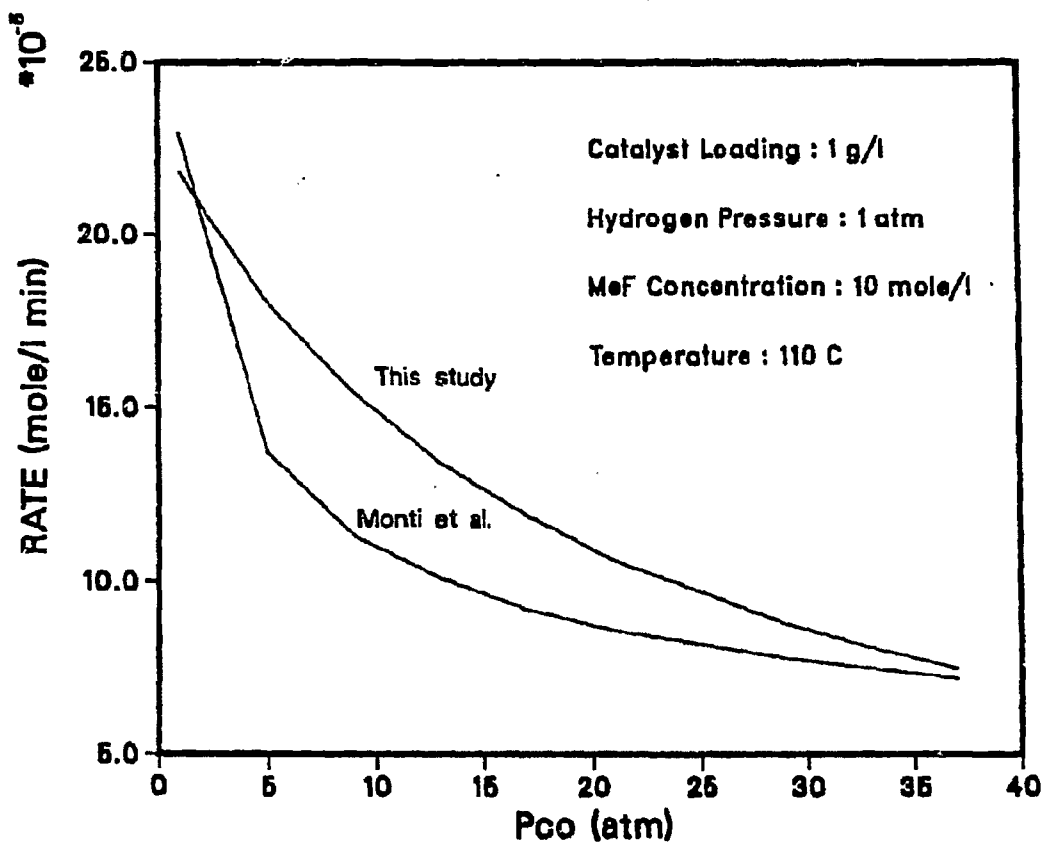
Figure 4. Effect of CO on hydrogenolysis of methyl formate as found in this work and as reported by Monti et al.

are much faster than the hydrogenolysis rate at the same temperature. The rate limited step in the case of simultaneous two-step reactions would be the hydrogenolysis.

Table 2

Variation of Rate Constants with Temperature

| Temp. | Carbonylation | | Hydrogenolysis |
	k	k$^-$	k
100	0.000032	0.0014	0.00000018
120	0.000265	0.0477	0.00000105
140	0.000924	0.3774	0.00000296
160	0.002868	2.4675	0.00000758

k : rate constant for forward reaction
k$^-$: rate constant for reverse reaction

The kinetic information obtained in this study indicates that carrying out the two reactions in a single reactor has the disadvantage that the reactor cannot be operated at optimum condition for both reactions at the same time. Severe problems would be equilibrium limitation of carbonylation and low reaction rate of hydrogenolysis.

Future Work

During the next quarter, work will emphasize experimental study of simultaneous two-step reactions in a single-stage slurry reactor.

Bibliography

1. Aguilo, A. and Horlenko, T., *Hydrocarbon Processing*, Nov. (1980)

2. Christiansen, J.A., U. S. Patent, 1,302,011 (1919).

3. Klier, K., *Catalysis of Organic Reaction*, edited by William R. Moser, Marcel Dekker, Inc. (1981).

4. Lee, S., Research to Support Development of the Liquid-Phase Methanol Synthesis Process, Interim Report (1986) Electric Power Research Inst.; Palo Alto, CA.

5. Monti, D.M., Kohler, M.A., Wainwright, M.S., Trimm, D.L. and Cant, N.W., *Applied Catalysis*, 22, (1986).

6. Sorum, P.A. and Onsager, O.T., *Proc. of 8th Int. Congr. on Catal.*, Berlin (1984).

7. Tonner, S.P., Trimm, D.L., Wainwright, M.S., and Cant, N.W., *J. of Molecular Catalysis*, 18 (1983).

Task 2: Coal Liquefaction under Supercritical Conditions

Supercritical fluid extraction is an attractive process primarily because the density and solvent power of a fluid changes dramatically with pressure at near critical conditions, and during the extraction of coal, the density of a supercritical fluid should also change the extractability of the coal. During earlier quarters a non-reacting supercritical fluid, toluene, was studied to determine the effect of density of the coal extraction/reaction process. Extractions were carried out for 2 to 60 minutes at reduced densities between 0.5 and 2.0 and at temperatures between 647 and 698 K. The data obtained can be explained by the hypothesis that coal dissolution is required preceding liquefaction reactions and that the degree of dissolution depends upon solvent density and temperature. A kinetic model shows that higher solvent densities result in faster conversion rates and in higher total conversions. Two papers have resulted from this study.

A second factor that makes supercritical extraction attractive is high mass transfer rates. At high pressures, mass transfer rates in a supercirital fluid are much higher than in a liquid, despite the fact that the supercritical fluid has liquid-like solvent powers. The objective of this work is to measure mass transfer rates for naphthalene extraction by carbon dioxide to enable us to determine how mass transfer coefficients vary with pressure, flow rate, and bed height, since these parameters will influence the design of extraction or reaction processes which utilize supercritical fluids. Ultimately, such measurement will be extended to coal/supercritical fluid systems to help define the flow rates liquid/solvent ratios that would be appropriate for a supercritical system.

Review of Mass Transfer/Equilibrium Under Supercritical Consitions

Over the past few years, significant interest has been expressed in a separation concept wherein a condensed phase (liquid or solid) is contacted with a fluid phase that is supercritical both in a temperature and pressure sense. Several industrial extraction processes have been developed such as deasphalting petroleum with supercritical propane (1) and decaffeinating coffee with supercritical carbon dioxide (2). Other examples would include deashing coal liquids (3) and regenerating activated carbon with carbon dioxide (4).

Supercritical carbon dioxide is a particularly attractive solvent for practical applications because it is nontoxic, nonflammable, environmentally acceptable, and relatively inexpensive. The critical temperature of carbon dioxide is only 304 K and thus extractions can be accomplished at moderate temperatures where thermal degradation of heat-labile extracts is minimal.

One of the cited advantages for using supercritical fluids as extractants is that the diffusion coefficients are significantly higher than for liquid systems while the viscosity more closely approximates that of a gas. Such trends would lead one to conclude that mass transfer charactersitics of supercritical fluids may be better than for comparable extractions carried out in the normal liquid phase.

There are few experimental data for diffusion coefficients of solutes in supercritical fluids. Those available are shown in Figure 5 where diffusion coefficients are plotted as a function of reduced pressure of the solvent gases for the systems CO_2-napthalene, CO_2-benzene, and ethylene-napthalene. The low-pressure data show D_{AB} to be inversely proportional to pressure, but, approximately, $D_{AB} \alpha P^{1/2}$. The range of reduced temperatures shown in Figure 5 is 0.97 to 1.09. At higher temperatures, D_{AB} would increase.

There is an interesting discontinuity in Figure 5 for the system CO_2- napthalene at 35^oC. At a pressure of about $80 \sim 81$ bar ($P_r \sim 1.09$), the lower critical end point is attained and the diffusion coefficient is essentially zero (5). The change in D_{AB}, as this critical point is approached, is very abrupt. Diffusion coefficients have not been reported for systems near the upper critical end points, but judging from the general trend of liquid-liquid systems near critical points (6, 7), it would be expected that diffusion coefficients would be very small in this region. In general, even though one has few data, it would appear that the binary diffusion coefficients for solutes in supercritical gases are around 10^{-4} cm^2/s for P_r values of $1 \sim 5$ and T_r values of $1 \sim 1.2$.

In the pressure and temperature range where most supercritical extractions would be operated, there are no generally accepted correlations for mass transfer coefficients. Storck and Coeuret (8) and Wilson and Geankoplis (9) have reviewed liquid phase relations while Gupta and Thodos (10) cover dilute gas phase systems. Both Bradshaw and Bennett (11) and Pfeffer (12) point out that due to the difference in Schmidt numbers, liquid and gases would be expected to have different correlations for the mass transfer coefficient.

It is the purpose of this work to measure mass transfer coefficients and to compare their dependence on pressure and temperature to the corresponding dependence of diffusion coefficients. In this way, the relationship between diffusion coefficients and mass transfer coefficients can be determined.
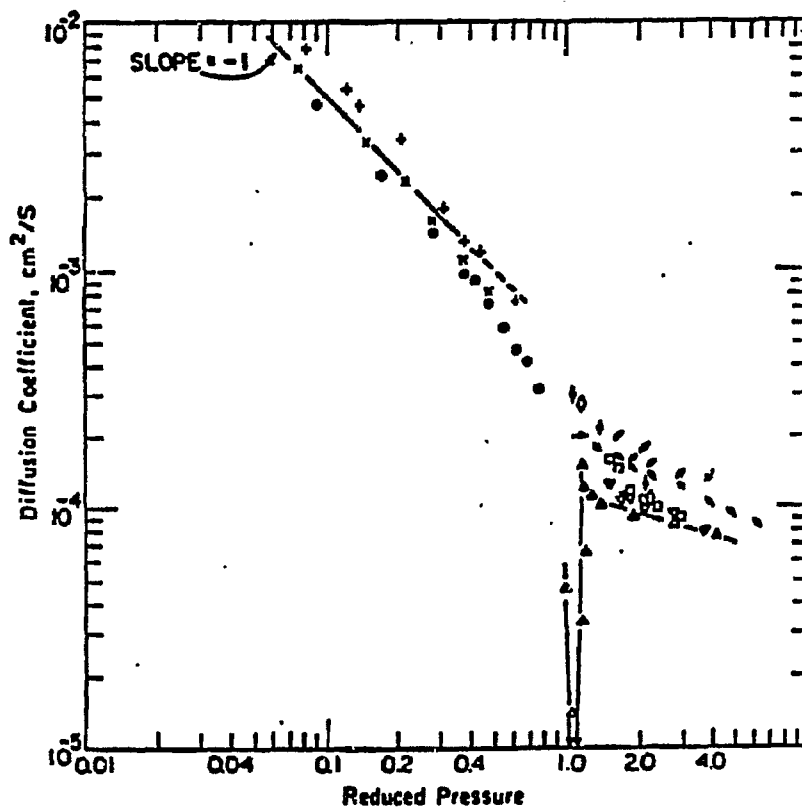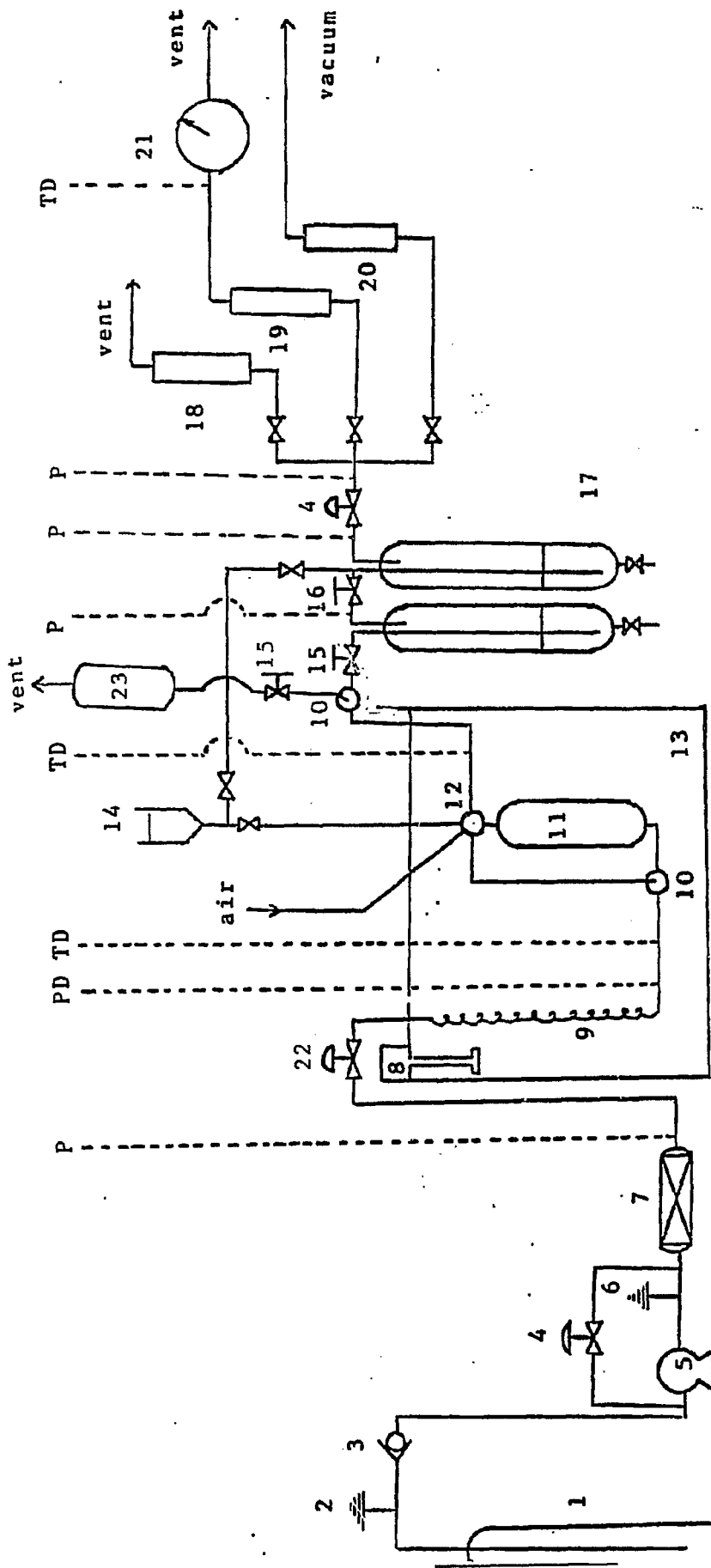
Fig. 5 The Diffusion Coefficients in Supercritical Fluids

Experimental Design

The schematic diagram of the experimental apparatus used in the past quarter is shown in Figure 6. Liquid carbon dioxide is pumped into the system via a high-pressure Milton-Roy liquid pump. Pressure is controlled by using a back pressure regulator and pressure fluctuations are dampened with an on-line surge tank. The system consists of a preheater which allows the solvent to reach the desired temperature and the extraction vessel 313 cm^3 in volume, 26.67 cm in length and 3.87 cm in diameter. The extraction vessel is packed with napthalene pellets which have been made from pure napthalene using a die. The height of the packing in the bed can be changed by using inert packing at the bottom and the top of the bed. The inert packing material being used is glass beads with size similar to that of the pellets. Another advantage in using the inert pellets is to get rid of end effects in the packed bed being used as the extractor. Pressure at the inlet of extractor is measured using a pressure transducer. The temperature of the extractor is measured at the inlet and outlet.

The fluid mixture coming out of the extractor is depressurized to atmospheric pressure by passing it through a heated metering valve and a back pressure regulator (4). The instantaneous flow rate of the gas leaving the extractor is measured using a rotameter and the total amount of gas flow is measured with a calibrated wet test meter. During this quarter, the bypass line has been modified as explained below.

The mass of precipitated solid will be found as described below. With this value and total amount of gas flow from wet test meter, the mole fraction of solids in the supercritical fluid can be readily determined. The inlet stream temperature and pressure of wet test meter are also measured.

1. Cylinder
2. Relief valve
3. Check valve
4. Back pressure regulator
5. Liquid pump
6. Relief valve
7. Surge tank

8. Temperature controller
9. Preheater
10. Three-way valve
11. Extractor
12. Five-way valve
13. Water bath
14. Solvent(Toluene) tank

15. Metering valve
16. Metering valve
17. Sample tanks
18. Rotameter
19. Rotameter
20. Rotameter
21. Wet test meter
22. Pressure Regulator
23. Naphthalene trap

P: Pressure gauge
PD: Pressure transmitter to Data logger
TD: Thermocouple to Data logger

Fig. 6 Schematic Diagram of the Experimental Apparatus for Supercritical Fluid Extraction

In the present system, the sample collectors are high pressure bombs which are kept at room temperature by two 200 watt resistance heaters. Each vessel contains toluene which will help dissolve the extract (napthalene) from the CO_2. These vessels are operated at 300 to 400 psia where the solubility of the solid in the CO_2 is at a minimum. The second vessel is redundant and is used to guarantee that all of the extract is collected and to reduce entrainment losses. No napthalene was found in these vessels during current experiments.

To determine the amount of extract collected, the amount of toluene (with dissolved extract) will be weighed. A sample of the toluene-extract solution will then be injected into a gas chromatograph to determine what portion of the solution is extract. To insure no extract remains in the line between valve 12 and the sample cylinder, valve 12 was converted to a five-way valve to allow washing of the line with toluene. Finally, the bypass, from valve 10 to 12, is designed to insure steady flow before allowing the CO_2 to pass through the extraction vessel (11).

The whole apparatus is rated for a pressure of 5,000 psi. All measured temperatures and pressures are recorded on a data logger.

The parameters that are being studied are:

    a.   effect of flow rate on solubility of napthalene in carbon dioxide at different pressures and temperatures;

    b.   effect of bed height on the mass transfer coefficient under supercritical conditions;

    c.   effect of flow rate on the mass transfer coefficient under supercritical conditions;

    d.   effect of pressure on the mass transfer coefficient under supercritical conditions.

The experimental conditions are as follows:

  System: Napthalene – Carbon dioxide

  Pellet characteristics:

      Material: Napthalene

      Shape: Cylindrical

      Size: Length (mm) = 4.5

                 Diameter (mm) = 4.5

  Height of Bed (cm): 13.3, 8.9, 6.7

  Temperature of Bed (^{O}K): 298, 308, 328

  Pressure (psi): 1470, 2205, 2940, 3675

  Flow rate (Std. Lit/Min at $70^{O}F$ and 1 atm): 4 ~ 40

Calculation of Mass Transfer Coefficients

The measurement of mass transfer coefficients is based upon the following equation:

The mass transfer coefficient is calculated as:

$$Ky = (\frac{\overline{G_{My}}}{a \, Z_T}) \, \ln (\frac{Y_A^*}{Y_A^* - Y_{out}}) \tag{1}$$

where $\overline{G_{My}}$ is the averaged molal mass velocity of the gas in moles per unit area per unit time.

where Y_A* is equilibrium mole fraction and Z_T is the height of the packed section, and a is the interfacial gas/solid area per unit volume.

Y_{out} can be determined by the amount of napthalene precipitated and total amount of carbon dioxide passed through the experimental apparatus during the given time.

$$Y_{out} = \frac{N_{C_{10}H_8}}{N_{C_{10}H_8} + N_{CO_2}}$$

$$N_{C_{10}H_8} = \frac{W_{C_{10}H_8}}{Mol. Wt. (128)}, \quad N_{CO_2} = \frac{PV}{ZRT}, \quad (Z = 0.995)$$

Work for Current Period

The schematic diagram shown in Figure 6 was built and tested for supercritical conditions. In this experiment, the solid dissolved in vessel (11), under supercritical conditions, was precipitated in and plugged the pipe line following metering valve (15). This plugging problem occurred because the amount of solid dissolved into CO_2 gas under supercritical condition was much larger (above 100 times) than that under the subcritical condition (308°K, 20 atm) of previous experiments. For pressures above 100 atm, the pressure drop through the metering valve (5) for bypass (between valve 10 and solid trop 23) was high and metering valve (15) was so sensitive that the pressure in the extractor (11) fluctuated significantly.

In the revised system Figure 7, we made the size of the pipe line following the metering valve larger (1/8" → 1/4"), and the solid trap (20) was connected to a back pressure regulator (22) to eliminate the fluctuation of pressure in extractor (11).

After revising our system, we operated it for 20 minutes at 308°K and 100 atm for several flow rates. After analysis of our samples, we have found that

1. Cylinder
2. Relief valve
3. Check valve
4. Liquid pump
5. Back pressure regulator
6. Surge tank
7. Pressure regulator
8. Temperature controller

9. Preheater
10. Three-way valve
11. Extractor
12. Three-way valve
13. Three-way valve
14. Water bath
15. Solvent tank
16. Four-way valve

17. Metering valve
18. Sample tanks
19. Metering valve
20. Solid trap
21. Three-way valve
22. Back pressure regulator
23. Rotameter
24. Wet test meter

P: Pressure gauge
PD: Pressure transmitter to Data logger
TD: Thermocouple to Data logger

Fig. 7 Schematic Diagram of the Experimental Apparatus for Supercritical Fluid Extraction

several samples at low flow rate reached equilibrium solubility and no solid napthalene remained in the extractor (11) after several runs. These results come from the fact that the solid napthalene dissolves into CO_2 gas so rapidly under supercritical conditions. During the next quarter, we are going to decrease the running time to about 5 minutes and increase the flow in order that less naphthalene dissolves. This will allow accurate mass transfer coefficients to be obtained.

References to Task 2

(1)   Zhuze, T.P.; Petroleum (London) (1960), 23, 298.

(2)   Vitzthum, O.; Hubert, P. German Patent 23575PO, (1975).

(3)   Baldwin, R.S.; Davis, R.E.; Wing, H.F. "Critical Solvent De-Ashing – A
      New Solids Separation Method for Coal Liquefaction Processes," presented
      at the 4th International Conference on Coal Gasification, Liquefaction,
      and Conversion to Electricity, University of Pittsburgh, Pittsburgh, PA,
      Aug. 1977.

(4)   Modell, M.; deFillippl, R.P.; Krukomis, V.J. "Regeneration of Activated
      Carbon with Supercritical Carbon Dioxide," presented at the National
      Meeting of American Chemical Society, Miami, FL Sept. 14, 1978.

(5)   Tsekhanskaya, Yu.V., Diffusion of Napthalene in Carbon Dioxide Near the
      Liquid-Gas Critical Point, Russ. J. Phys. Chem., 45, 744 (1971).

(6)   Ramie, R.W. and Cussler, E.L., Fas Fluxes with Supercritical Sovlents,
      AIChE J., 20, 353-356 (1974).

(7)   Tsekhanskaya, Yu.V., Diffusion in the System p-Nitrophenol-Water in the
      Critical Region, Russ. J. Phys. Chem. 42, 532-3 (1968).

(8)   Storck, A. and Coeuret, F., Mass Transfer Between a Flowing Fluid and a
      Wall or Immersed Surface in Fixed and Fluidized Beds, Chem. Eng. J., 20,
      149-56 (1980).

(9)   Wilson, E.J. and Geankoplis, C.J., Liquid Mass Transfer at Very Low
      Reynolds Numbers in Packed Beds, Ind. Eng. Chem. Fund., 5, 9-14 (1966).

(10) Gupta, A.J. and Thodos, G., Mass and Heat Transfer in the Flow of Fluids
      Through Fixed and Fluidized Beds of Spherical Particles, AIChE J., 8,
      608-10 (1962).

(11) Bradshaw, R.D. and Bennett, C.O., Fluid-Particle Mass Transfer in a
      Packed Bed, AIChE J. 7, 48-52 (1961).

(12) Pfeffer, R., Heat and Mass Transport in Multiparticle Systems, Ind. Eng.
      Chem. Fund., 3, 380-3 (1964).